CrossMark

High Power Laser Science and Engineering, (2021), Vol. 9, e39, 7 pages.
doi:10.1017/hpl.2021.26

HIGH POWER LASER SCIENCE AND ENGINEERING

RESEARCH ARTICLE

Utilizing phase-shifted long-period fiber grating to suppress spectral broadening of a high-power fiber MOPA laser system

Yinxu Bian[1,2], Kerong Jiao[1,2], Xuecheng Wu[1,2], Hua Shen[1,2,3], Feiyan Yang[1,2], and Rihong Zhu[1,2]

[1]*School of Electronic Engineering and Optoelectronic Technology, Nanjing University of Science and Technology, Nanjing 210094, China*

[2]*MIIT Key Laboratory of Advanced Solid Laser, Nanjing University of Science and Technology, Nanjing 210094, China*

[3]*Department of Material Science and Engineering, University of California Los Angeles, Los Angeles, CA 90095, USA*

(Received 30 November 2020; revised 19 April 2021; accepted 29 April 2021)

Abstract

Suppressing nonlinear effects in high-power fiber lasers based on fiber gratings has become a hotspot. At present, research is mainly focused on suppressing stimulated Raman scattering in a high-power fiber laser. However, the suppression of spectral broadening, caused by self-phase modulation or four-wave mixing, is still a challenging attribute to the close distance between the broadened laser and signal laser. If using a traditional fiber grating with only one stopband to suppress the spectral broadening, the signal power will be stripped simultaneously. Confronting this challenge, we propose a novel method based on phase-shifted long-period fiber grating (PS-LPFG) to suppress spectral broadening in a high-power fiber master oscillator power amplifier (MOPA) laser system in this paper. A PS-LPFG is designed and fabricated on 10/130 passive fiber utilizing a point-by-point scanning technique. The resonant wavelength of the fabricated PS-LPFG is 1080 nm, the full width at half maximum of the passband is 5.48 nm, and stopband extinction exceeds 90%. To evaluate the performance of the PS-LPFG, the grating is inserted into the seed of a kilowatt-level continuous-wave MOPA system. Experiment results show that the 30 dB linewidth of the output spectrum is narrowed by approximately 37.97%, providing an effective and flexible way for optimizing the output linewidth of high-power fiber MOPA laser systems.

Keywords: fiber optics component; high-power fiber laser; nonlinear effects; phase-shifted long-period fiber grating; spectral broadening

1. Introduction

High-power fiber lasers are import to several applications such as industrial manufacturing[1,2], astronomy[3], and beam combination[4-6]. Currently, the master oscillator power amplifier (MOPA) configuration has become a widely used choice to realize high-power output[7-10]. However, with the increase of the output power, the main signal laser's spectra will be broadened drastically by nonlinear effects such as self-phase modulation (SPM)[11-13] and four-wave mixing (FWM)[11,14], which significantly affect the stability and further power improvement of the laser.

At present, utilizing a special fiber grating to suppress nonlinear effects has become a hot topic by virtue of the characteristics of waveband selection and natural compatibility with fiber. However, most researchers have focused on suppressing stimulated Raman scattering (SRS) in fiber lasers utilizing chirped and tilted fiber Bragg gratings (CTFBGs) or long-period fiber gratings (LPFGs). CTFBGs can couple the Raman light from forward-propagating core modes to backward-propagating cladding modes, which can be regarded as a broadband tunable band-stop filter[15]. In 2017, Wang *et al.*[16,17] first fabricated a CTFBG to suppress SRS in a fiber amplifier. Then, they used cascading multiple CTFBGs to suppress SRS in a 5-kW fiber laser[18-20]. In 2019, we enabled CTFBG to work well at over 1-kW laser power and applied it to suppress SRS in a kilowatt-level continuous-wave (CW) fiber laser whose SRS was suppressed by 99.5%[21]. Similarly, LPFGs can suppress

Correspondence to: H. Shen, MIIT Key Laboratory of Advanced Solid Laser, Nanjing University of Science and Technology, Nanjing 210094, China. Email: edwardbayun@163.com

© The Author(s), 2021. Published by Cambridge University Press in association with Chinese Laser Press. This is an Open Access article, distributed under the terms of the Creative Commons Attribution licence (http://creativecommons.org/licenses/by/4.0/), which permits unrestricted re-use, distribution, and reproduction in any medium, provided the original work is properly cited.

https://doi.org/10.1017/hpl.2021.26 Published online by Cambridge University Press

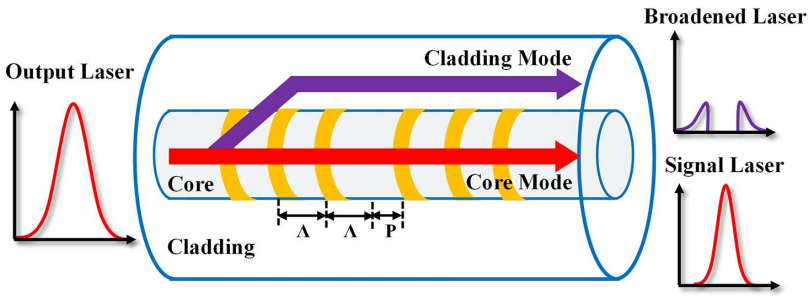

Figure 1. Schematic diagram of the structure of PS-LPFG. When the output laser transmits through the PS-LPFG, the broadened laser will be coupled from the core to the cladding and the signal laser continues to transmit.

SRS by coupling the Raman scattered light from forward-propagating core modes to forward-propagating cladding modes. In 2011, Nodop *et al.* inserted LPFGs into the gain fiber of a pulsed fiber laser[22]. The experimental results showed that LPFGs can effectively suppress SRS in a pulsed fiber laser. In 2020, we utilized LPFGs to suppress SRS in the seed and amplifier of a kilowatt-level MOPA system separately[23]. It is well known that the distance between the wavelength of the Raman light and the wavelength of signal laser is over dozens of nanometers, which means SRS is an independent spectrum. Therefore, it is feasible to utilize the continuous stopband of CTPFGs or LPFGs to filter the Raman light, whereas the signal light will not be stripped. However, the spectral broadening caused by SPM and FWM is distributed symmetrically around the signal laser by several nanometers[11,13]. If we use existing CTFBGs or LPFGs to filter the broadened spectrum, it will definitely weaken the signal power dramatically. Therefore, it is a great challenge to optimize the spectrum of the main signal laser by filtering the broadened laser.

To suppress the spectral broadening produced by SPM and FWM, we first propose to utilize a phase-shifted (PS)-LPFG to filter the broadened spectrum and apply it in a high-power MOPA system. We design and fabricate a PS-LPFG on a passive 10/130 fiber utilizing the point-by-point ultraviolet (UV) inscribing technique. The resonant wavelength of the PS-LPFG is 1080 nm, the full width at half maximum (FWHM) of the passband is 5.48 nm, and the stopband extinction exceeds 90%. To substantiate the feasibility of our method, the PS-LPFG is inserted into the seed of a 1080 nm MOPA system to suppress spectral broadening aroused by the oscillating seed. The spectral linewidth of the kilowatt-level fiber laser is narrowed significantly (the 30 dB linewidth is narrowed by approximately 37.97%), and the slope efficiency of the fiber laser is increased slightly.

2. Simulations

As shown in Figure 1, PS-LPFG can be manufactured by introducing an unperturbed fiber with $\Lambda/2$ length (indicated by P) in the middle of an LPFG, where Λ is the period of LPFG. Similar to LPFG, the performance of spectral filtering could be adjusted by controlling the period of PS-LPFG, which can realize coupling a particular wavelength of light from forward-propagating core modes to forward-propagating cladding modes.

Previous research indicates that inserting a phase-shift into an LPFG can split the resonance of the LPFG and form two symmetrical resonances, as shown in Figure 2(a)[24,25]. The blue line of Figure 2(a) shows that a loss band can be achieved at the resonant wavelength of the LPFG because the transmittance reaches the minimum at the resonant wavelength. After inserting a π phase shift ($P = \Lambda/2$) in the center of an LPFG, the transmission spectrum changes obviously, as shown in the red line of Figure 2(a). Two new loss bands are generated on both sides of the original resonance wavelength of the LPFG, which constitutes a band-stop filter that can filter two wavelengths and simultaneously causes no loss at the original resonance wavelength. Therefore, through reasonable design, the passband of the PS-LPFG can match the signal laser, and the stopband can match the broadened laser which is stimulated by nonlinear effects. When the output laser passes through the PS-LPFG, the broadened laser will be coupled from the core to the cladding and the signal laser continues to transmit with low loss, as shown in Figure 1. This is the mechanism of suppressing spectral broadening of high-power fiber laser by utilizing the PS-LPFG.

Figure 2(b) shows the effect of the periods on the spectrum of the PS-LPFG. The central wavelength bathochromic shifts with the period of the PS-LPFG increase. According to this characteristic, we can control the period of the PS-LPFG to filter the broadened spectrum on both sides of the signal laser, equivalently suppressing the spectral broadening produced by nonlinear effects. Figure 2(c) shows the spectra of the PS-LPFG with different period numbers. The period of the PS-LPFG is 578 μm and index modulation amplitude is 8×10^{-5}. It can be observed that with the increasing of period numbers, the FWHM of the passband narrows, whereas the rejection depth increases. This characteristic is important for the filtering capacity of a PS-LPFG. As a result, we can adjust the period number of the PS-LPFG to match the broadened spectrum of the fiber laser. Furthermore, we simulate PS-LPFGs with different index modulation amplitudes

https://doi.org/10.1017/hpl.2021.26 Published online by Cambridge University Press

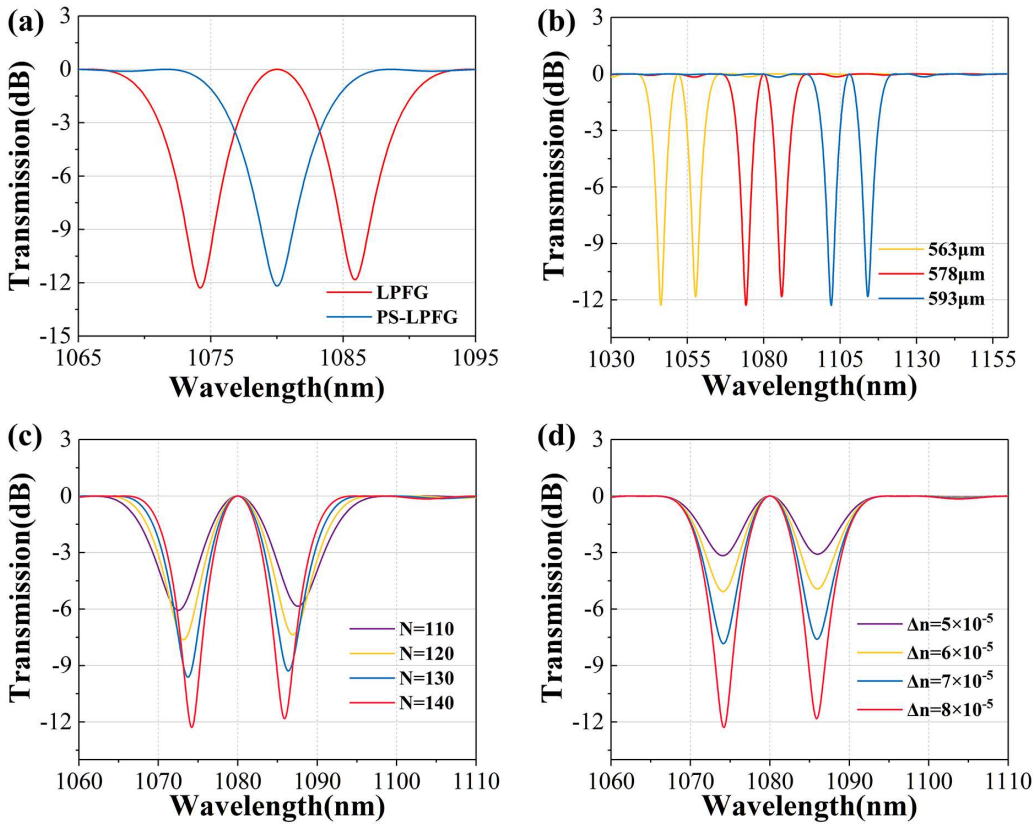

Figure 2. Simulated transmission spectrum of (a) LPFG and PS-LPFG with resonance wavelength 1080 nm at a period of 578 μm and a period number of 140; (b) PS-LPFGs with different periods at a period number of 140 and an index modulation amplitude of 8×10^{-5}; (c) PS-LPFGs with different period numbers at a period of 578 μm and an index modulation amplitude of 8×10^{-5}; and (d) PS-LPFGs with different index modulation amplitudes at a period of 578 μm and a period number of 140.

at the period 578 μm and the period number 140, as shown in Figure 2(d). Clearly, the index modulation amplitude has a great influence on the rejection depth of the transmission spectrum of the PS-LPFG. To change the index modulation amplitude of PS-LPFG, we can modify the hydrogenation pressure or time to achieve an appropriate photosensitivity of fibers. In addition, we can control the index modulation amplitude by adjusting the exposure time or the power of UV light during the fabrication of PS-LPFG.

According to the simulation results, after inserting a π phase shift in the center of an LPFG, two new loss bands are generated on both sides of the original resonance wavelength of the LPFG. We can set the period of PS-LPFG as 578 μm to be consistent with the wavelength of the evaluation system (1080 nm) in Section 4. Moreover, we choose a period number of 140 and index modulation amplitude of 8×10^{-5} to achieve the best effect of spectral linewidth optimization.

3. Fabrication

Figure 3 shows the point-by-point UV inscribing system with an online parameter measurement system. The CW UV inscribing beam with a wavelength of 244 nm and power of 25 mW is produced by the argon ion laser (Innova 90C FreD Ion Laser made by Coherent Corporation). The inscribing light is reflected by the UV mirror and then is incident to the UV cylindrical lenses. The cylindrical lens 1 compresses the UV light vertically to enhance the power density on the fiber, whereas the cylindrical lens 2 compresses the UV light horizontally to avoid the periodic overlap. The diameter of the UV spot is compressed to 120 μm by the dual cylindrical lenses. It is worth mentioning that the UV mirror, cylindrical lens 1, and cylindrical lens 2 are all fixed on the stepping motor. Therefore, the UV spot could move periodically along the direction of the fiber axis by controlling the stepping motor. To ensure that the focus center of the UV light could be located at the core of the fiber, the fiber is fixed on the six-dimensional translation stage. Before we inscribe the PS-LPFG, the two ends of the hydrogenated (to enhance the photosensitivity of the fiber core, 18 days at 13 MPa and 40°C) fiber (LMA-GDF-10/130-M, made by Nufern Corporation) are spliced to mode field adapters (MFAs). The laser generated by the amplified spontaneous emission (ASE) source is coupled into the inscribed fiber by MFA-1, and then coupled into an optical spectrum analyzer (OSA) by MFA-2, to monitor the spectral performance of the PS-LPFG in real time.

https://doi.org/10.1017/hpl.2021.26 Published online by Cambridge University Press

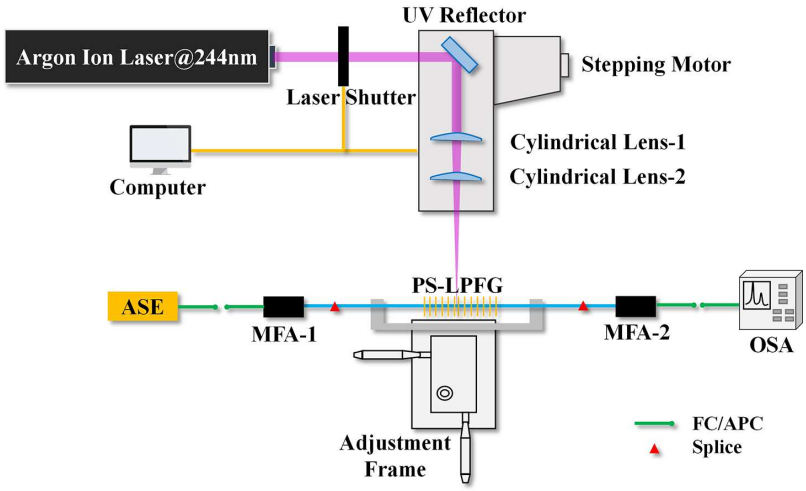

Figure 3. Inscribing system of PS-LPFG based on a point-by-point scanning technique.

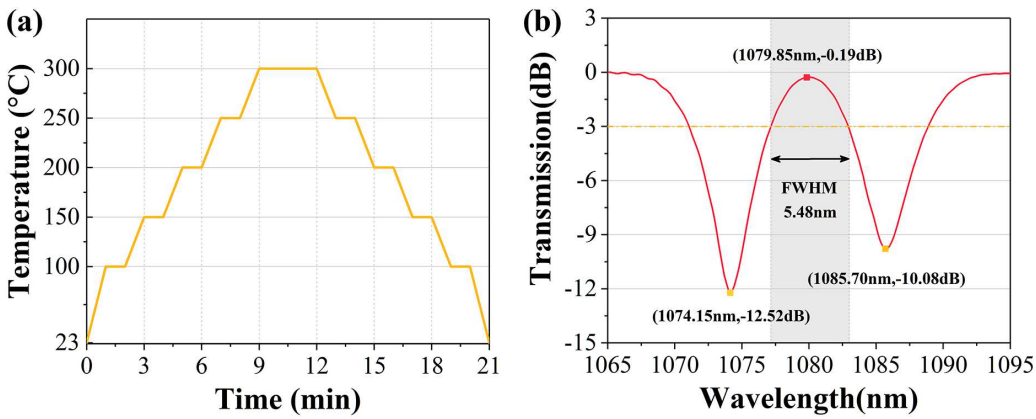

Figure 4. (a) Temperature curve of dynamic-high-temperature annealing and (b) transmission spectrum of the fabricated PS-LPFG after annealing.

During the process of lithography, the period of the PS-LPFG is 578 μm and the exposure time of each period is 15 s. After the exposure of one period, the computer controls the laser shutter to block the inscribing laser and the UV spot will scan to the next exposure position. Then the computer controls the shutter to open to inscribe the next period of PS-LPFG after confirming the position. This process will be repeated continuously until the UV spot arrives at the middle of the PS-LPFG. Then we change the scanning step from 578 to 867 μm (1.5Λ of the PS-LPFG) to insert a π phase shift in the middle of the PS-LPFG. Afterwards, the lithography period returns to 578 μm in the remainder of the lithography process. Furthermore, the spectral characteristics (center wavelength, FWHM, and extinction) of the PS-LPFG are time-varying. To guarantee the spectral performance of the PS-LPFG satisfies the requirement of suppressing the spectral broadening of the signal laser, an online measurement system is introduced into the inscribing system. Thus, we can immediately adjust the inscribing parameter according to the real-time feedback data. After fabrication of the PS-LPFG, there are a great number of residual dissociative hydrogen molecules and hydroxyl compounds formed by UV radiation inside the PS-LPFG[26]. These hydrogen molecules and hydroxyl compounds have great infrared absorption ability, resulting in heating or even burning of the PS-LPFG when kilowatt-level power passes through it. To promote the capacity of our PS-LPFG to carry high-power laser, our proposed dual annealing method is adopted[20,23]. The constant-low-temperature annealing (60°C for 30 days) is applied to volatilize the hydrogen molecules and the dynamic-high-temperature annealing is utilized to make the hydroxyl compounds be evaporated away from the PS-LPFG. Figure 4(a) shows the temperature curve of the dynamic-high-temperature annealing. Figure 4(b) shows the transmission spectrum of our PS-LPFG after annealing. It can be seen that the extinction of the stopbands is over 10 dB (90%) and the FWHM is 5.48 nm.

Moreover, attributed to its long period, the spectral performance of PS-LPFG is easily affected by the environment, which may decrease the inhibition effects. Therefore, a reduced-sensitivity packaging method, proposed in our

https://doi.org/10.1017/hpl.2021.26 Published online by Cambridge University Press

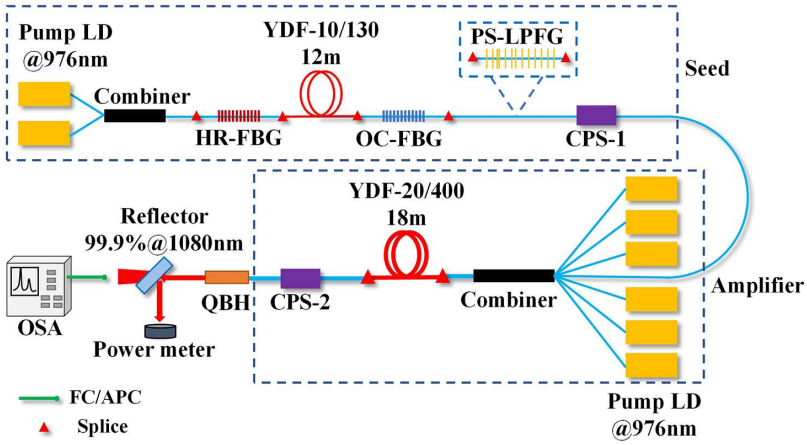

Figure 5. High-power MOPA system for evaluating performance of suppressing spectral broadening.

previous work[23], was also utilized on the grating to mitigate the environmental sensitivity of the PS-LPFG.

4. Experiments and results

Figure 5 shows the MOPA system for experimental verification of the spectral broadening suppression effect by our PS-LPFG. The seed with 84-W output power consists of two 976-nm pumps with 100-W output power, a 2 × 1 combiner, a resonant cavity, and a cladding power stripper (CPS-1). The resonant cavity is made up of a 12-m ytterbium-doped active fiber (LMA-YDF-10/130-M, made by Nufern Corporation) and a pair of 1080-nm fiber Bragg gratings (FBGs). The reflectivity of the high-reflection (HR)-FBG is 99.5% and that of the output-coupling (OC)-FBG is 10%. The FWHM of the HR-FBG is approximately 2.67 nm and that of the OC-FBG is approximately 1.14 nm. Furthermore, the pump module of the amplifier is composed of eight 976-nm pumps with 250-W output power and a (6 + 1) × 1 combiner. An 18-m ytterbium-doped active fiber (LMA-YDF-20/400-M, made by Nufern Corporation) is utilized as the gain medium. Then the amplified laser outputs via another CPS (CPS-2) and a quartz block of high power (QBH). An infrared reflector (reflectivity >99.9%) is placed along the 45° angle of the optical axis to reflect the output laser to the power meter. The transmitted light through the reflector is detected by the OSA to test the spectral curve of the high-power MOPA system. Our PS-LPFG is spliced between the OC-FBG and CPS-1, as shown in Figure 5. The optimization of the spectral broadening of signal power can be evaluated by measuring and comparing output spectra before and after inserting the PS-LPFG into the seed of the MOPA system.

Figure 6(a) shows the changing spectra of the output as the signal power increases without PS-LPFG. The phenomenon of spectral broadening of the signal laser caused by nonlinear effects can be clearly observed from the signal power of 102 W, and then becomes dramatically obvious with increasing signal power. To narrow the spectral linewidth of the output power, we spliced our PS-LPFG between OC-FBG and CPS-1 in the seed of the evaluation system, and the measured spectra of signal power are shown in Figure 6(b). It can be distinctly observed that the spectral broadening is well suppressed, especially in the long-wavelength direction. Figure 6(c) shows the comparison of the spectra without and with the PS-LPFG at the highest signal power. The blue line indicates the spectrum before splicing the PS-LPFG whereas the red line shows the spectrum after splicing the PS-LPFG. Meanwhile, we also separately list the linewidth of the two spectral curves and their difference of the linewidth of 3, 10, 13, 20, and 30 dB in Table 1.

Table 1. Linewidth of output laser before and after splicing the PS-LPFG (at maximum output power).

Position (dB)	Linewidth without PS-LPFG (nm)	Linewidth with PS-LPFG (nm)	Difference (nm)	Difference (%)
3	3.08	3.07	0.01	0.32
10	6.21	5.32	0.89	14.33
13	7.76	5.78	1.98	25.52
20	11.18	7.87	3.31	29.61
30	16.12	10.00	6.12	37.97

From the table, it can be calculated that the linewidth at 3 dB does not change significantly before and after PS-LPFG insertion. This is because the 3-dB linewidth of the passband of the PS-LPFG is about 5.48 nm, which is larger than the linewidth of the signal laser at the 3-dB position, so that the signal laser at the 3-dB position can pass through the PS-LPFG with low loss. Compared with the 3-dB position, the linewidth optimization ratio at 10 dB is more obvious, and the linewidth at 10 dB is reduced from 6.21 to 5.32 nm (narrowed by 14.33%), because nonlinear effects have already affected the 10 dB linewidth of the output spectrum. However, limited by the linewidth of the passband of the PS-LPFG, the grating can only couple part of the broadened laser to the cladding and make it stripped by the CPS. To further optimize the output spectral linewidth at

https://doi.org/10.1017/hpl.2021.26 Published online by Cambridge University Press

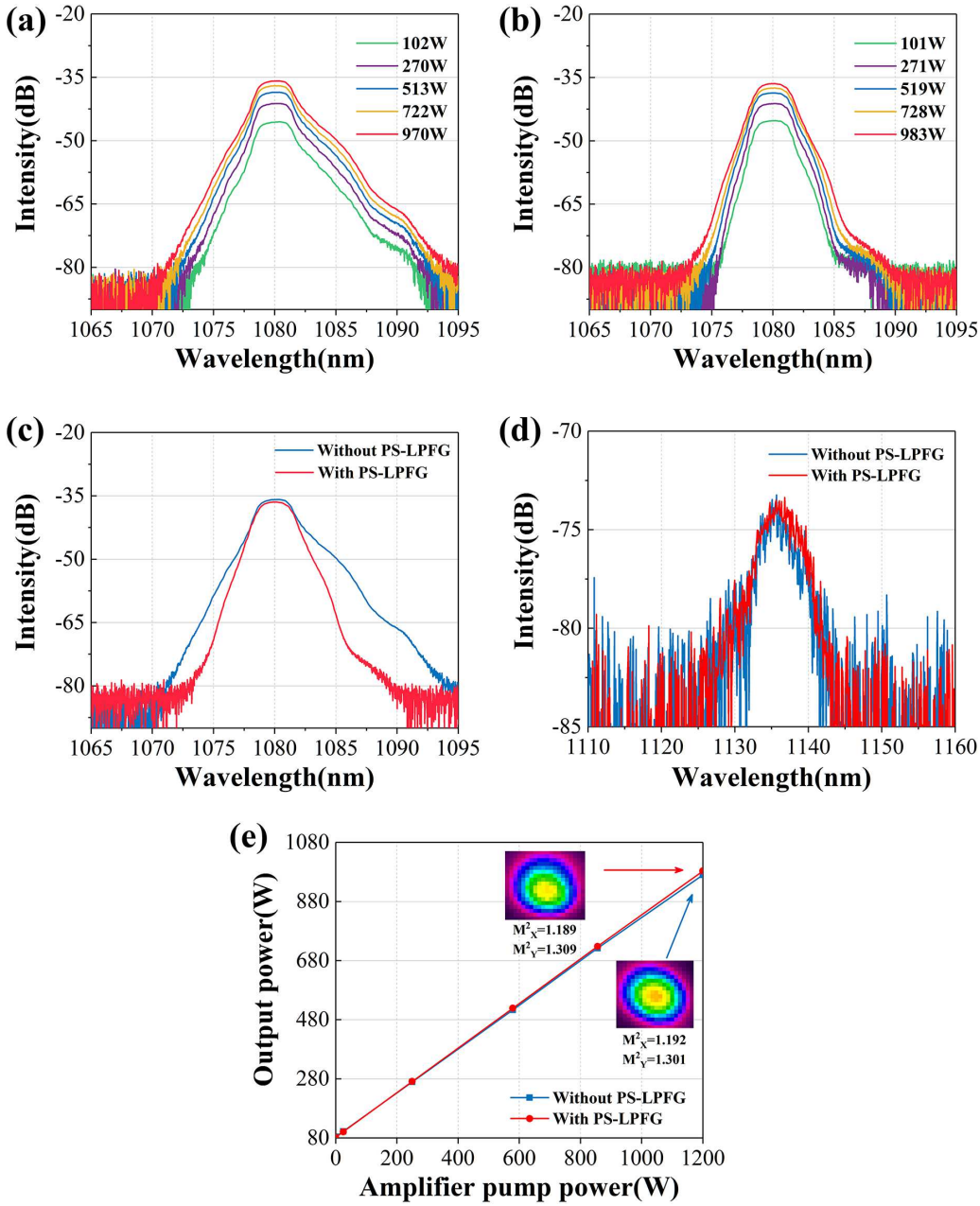

Figure 6. Output spectra of the evaluation system (a) without and (b) with PS-LPFG and comparison of the output spectra with and without the PS-LPFG at the highest power (c) in the range of signal laser and (d) in the range of SRS, and (e) output power versus pump power without or with PS-LPFG with the beam quality and profile of the output.

3-dB and 10-dB positions, we need to increase the length of the PS-LPFG to narrow the linewidth of the passband of the grating. As for the 13-dB position, the linewidth is reduced from 7.76 to 5.78 nm (narrowed by 25.5%). The linewidth at 20 dB is reduced from 11.18 to 7.87 nm (narrowed by 29.61%) and the linewidth at 30 dB is reduced from 16.12 to 10.00 nm (narrowed by 37.97%). Therefore, it can be concluded that our PS-LPFGs can exceptionally suppress the spectral broadening in kilowatt-level CW MOPA systems and, further, significantly optimize the linewidth level of the high-power fiber laser. We also measured the spectrum of SRS before and after inserting the PS-LPFG, as shown in Figure 6(d). The blue curve represents the spectrum of Stokes light without PS-LPFG, and the red curve shows that of Stokes light with PS-LPFG. It can be obviously observed that there is no evident change in spectrum of the SRS before and after inserting the PS-LPFG. This is because our PS-LPFG has no resonance in the range of SRS, so the Stokes light cannot be filtered out from the fiber core.

Figure 6(e) shows the slope efficiency of the evaluation system with and without PS-LPFG. It is worth mentioning that the slope efficiency of the MOPA system increases

https://doi.org/10.1017/hpl.2021.26 Published online by Cambridge University Press

slightly after inserting the PS-LPFG. The slope efficiency of the evaluation system is approximately 73.83% before inserting the PS-LPFG and approximately 75.08% after. The reason for this increase could be explained by the PS-LPFG filters broadening the laser from the output signal of the seed filtering out the spectra of the seed laser at the long-wavelength zone, in other words, reducing the quantum defect of the pump power converting it into a laser of longer wavelength in the amplifier[18]. We further measured the M^2 factor of the evaluation system before and after inserting the PS-LPFG and the experimental results are shown in Figure 6(e). Before the PS-LPFG is connected, M_X^2 and M_Y^2 of the output laser are approximately 1.192 and 1.301, respectively, when the output power reaches the maximum. After PS-LPFG is connected, M_X^2 and M_Y^2 of the output laser are approximately 1.189 and 1.309, respectively. It can be observed from the experimental results that there is almost no variation in the beam quality before and after inserting the PS-LPFG. Although PS-LPFG couples part of the broadened laser to the cladding, this part of the cladding light is stripped by the CPS. Therefore, PS-LPFG will not affect the beam quality of the system.

5. Conclusion

Attributed to the spectral characteristics of the PS-LPFG of one passband with two symmetric stopbands, it is feasible to utilize a PS-LPFG to suppress the spectral broadening produced by nonlinear effects. Simultaneously, a PS-LPFG can be conveniently applied in fiber lasers owing to its natural compatibility with the fiber, which means it could be a universal method to optimize the output linewidth of high-power fiber lasers. In this paper, a PS-LPFG with 1080 nm resonant wavelength, 5.48 nm FWHM, and 90% stopband extinction was designed and fabricated by using a point-by-point UV inscribing method. This is the first utilization of a PS-LPFG in the seed of a MOPA system to suppress spectral broadening of the main signal laser. Experiment results demonstrated that the spectral linewidth is obviously optimized (30 dB bandwidth narrowed by 37.97%) at a kilowatt-level signal power and the slope efficiency of the laser is improved slightly. As proved by the results, our PS-LPFG is a feasible solution to suppressing nonlinear effects such as SPM and FWM in high-power fiber lasers, providing a universal and effective way to optimize the output linewidth of high-power fiber lasers.

Acknowledgments

This work was supported by the National Key Research and Development Program of China (No. 2017YFB1104402), the Pre-research Foundation of Equipment Development Department (No. 61404140105), the Key Laboratory of Optical System Advanced Manufacturing Technology of the Chinese Academy of Sciences (No. KLOMT190101), the Jiangsu Provincial Key Research and Development Program (No. BE2019114), the Basic Research Program of Jiangsu Province (No. BK20190456), and the National Natural Science Foundation of China (No. 62005120).

References

1. Y. B. Wang, G. Chen, and J. Y. Li, High Power Laser Sci. Eng. **6**, e40 (2018).
2. L. D. Scintilla and L. Tricarico, Opt. Eng. **52**, 076115 (2013).
3. A. Buikema, F. Jose, S. Augst, P. Fritschel, and N. Mavalvala, Opt. Lett. **44**, 3833 (2019).
4. C. Wirth, O. Schmidt, I. Tsybin, T. Schreiber, R. Eberhardt, J. Limpert, A. Tünnermann, K. Ludewigt, M. Gowin, E. Have, and M. Jung, Opt. Lett. **36**, 3118 (2011).
5. Y. Zheng, Y. Yang, J. Wang, M. Hu, G. Liu, X. Zhao, X. Chen, K. Liu, C. Zhao, B. He, and J. Zhou, Opt. Express **24**, 12063 (2016).
6. Y. Zheng, Z. D. Zhu, X. X. Liu, M. Yu, S. Y. Li, L. Zhang, Q. L. Ni, J. L. Wang, and X. F. Wang, Appl. Opt. **58**, 8339 (2019).
7. Y. Jeong, J. Nilsson, J. K. Sahu, D. N. Payne, R. Horley, L. M. B. Hickey, and P. W. Turner, IEEE J. Sel. Topics Quantum Electron. **13**, 546 (2007).
8. J. P. Hao, H. Zhao, D. Y. Zhang, L. M. Zhang, and K. Zhang, Appl. Opt. **54**, 4857 (2015).
9. J. Xu, W. Liu, J. Leng, H. Xiao, S. Guo, P. Zhou, and J. Chen, Opt. Lett. **40**, 2973 (2015).
10. Y. S. Huang, Q. R. Xiao, D. Li, J. T. Xin, Z. H. Wang, J. D. Tian, Y. L. Wu, M. L. Gong, L. Q. Zhu, and P. Yan, Opt. Laser Technol. **133**, 106538 (2021).
11. G. P. Agrawal, *Nonlinear Fiber Optics* (Academic, UK, 2013).
12. F. Beier, C. Hupel, S. Kuhn, S. Hein, J. Nold, F. Proske, B. Sattler, A. Liem, C. Jauregui, J. Limpert, N. Haarlammert, T. Schreiber, R. Eberhardt, and A. Tünnermann, Opt. Express **25**, 14892 (2017).
13. S. I. Kablukov, E. A. Zlobina, E. V. Podivilov, and S. A. Babin, Opt. Lett. **37**, 2508 (2012).
14. Z. H. Huang, X. B. Liang, C. Li, H. Lin, Q. Li, J. Wang, and F. Jing, Appl. Opt. **55**, 297 (2016)
15. F. Liu, T. Guo, C. Wu, B. O. Guan, C. Lu, H. Y. Tam, and J. Albert, Opt. Express **22**, 24430 (2014).
16. M. Wang, Y. J. Zhang, Z. F. Wang, J. J. Sun, J. Q. Cao, J. Y. Leng, X. J. Gu, and X. J. Xu, Opt. Express **25**, 1529 (2017).
17. M. Wang, Z. X. Li, L. Liu, Z. F. Wang, X. J. Gu, and X. J. Xu, Appl. Opt. **57**, 4376 (2018).
18. M. Wang, Z. F. Wang, L. Liu, Q. H. Hu, H. Xiao, and X. J. Xu, Photonics Res. **7**, 167 (2019).
19. X. Tian, X. Zhao, M. Wang, Q. Hu, H. Li, B. Rao, H. Xiao, and Z. Wang, Opt. Express **28**, 19508 (2020).
20. X. Tian, X. Zhao, M. Wang, and Z. Wang, Laser Phys. Lett. **17**, 085104 (2020).
21. K. R. Jiao, J. Shu, H. Shen, Z. W. Guan, F. Y. Yang, and R. H. Zhu, High Power Laser Sci. Eng. **7**, e31 (2019).
22. D. Nodop, C. Jauregui, F. Jansen, J. Limpert, and A. Tünnermann, Opt. Lett. **35**, 2982 (2010).
23. K. R. Jiao, H. Shen, Z. W. Guan, F. Y. Yang, and R. H. Zhu, Opt. Express **28**, 6048 (2020).
24. T. Erdogan, J. Lightwave Technol. **15**, 1277 (1997).
25. T. Erdogan, J. Opt. Soc. Am. A **14**, 1760 (1997).
26. B. W. Zhang and M. Kahrizi, IEEE Sens. J. **7**, 586 (2007).

https://doi.org/10.1017/hpl.2021.26 Published online by Cambridge University Press